Atmospheric and
Environmental Research, Inc.

Studies for the Europagenic Plasma Source in Jupiter's Inner Magnetosphere during the Galileo Europa Mission

ATMOSPHERIC AND ENVIRONMENTAL RESEARCH, INC.
LEXINGTON, MASSACHUSETTS

April 15, 2004

Atmospheric and
Environmental Research, Inc.

Studies for the Europagenic Plasma Source in Jupiter's Inner Magnetosphere during the Galileo Europa Mission

William H. Smyth

Atmospheric and Environmental Research, Inc.
131 Hartwell Avenue
Lexington, MA 02421-3126

Report for the Period of
February 19, 2002 to February 18, 2004

I. INTRODUCTION

The objective of this project as initially proposed was (1) to advance our understanding of the three-dimensional nature of the Europagenic plasma source (pickup ions created by electron impact ionization and charge exchange) near the satellite and its orbit, and (2) to elucidate its relationship to the upstream and downstream Galileo plasma and magnetic field measurements at the time of the Galileo Europa Mission (GEM) encounters with Europa. Significant progress has been made regarding the first part of this objective, as reported below, although this progress has been more difficult to achieve than initially projected. Because of the surprising observational discovery (Mauk et al. 2003) during this project of much larger circumplanetary populations of neutral clouds created by Europa than had ever previously been envisioned, the emphasis of the second part of this objective was largely and necessarily refocused to address this more major issue, which sets the larger context for the more local problem near the satellite. Nevertheless, most of the groundwork was completed to undertake the second part of the objective.

Research efforts reported here are therefore focused in three main areas: (1) improving the plasma torus description near Europa and its orbit about Jupiter, (2) implementing plasma-neutral chemistry in the neutral cloud model in order to undertake Europagenic plasma source studies, and (3) undertaking modeling studies for Europa's neutral clouds and their pickup ion production rates. A paper (Smyth and Marconi 2004) describing this research is in preparation.

II. PLASMA TORUS DESCRIPTION

Improvements of the plasma torus description in the neutral cloud models for Europa include the development and implementation of two factors: (1) an improved description of the trajectory of Europa about Jupiter that includes its actual non-circular and inclined orbital motions produced by multi-body gravitational interactions, and (2) an improved description of the offset-tilted dipole planetary magnetic field (for the plasma torus structure and properties about Jupiter near Europa's orbit) with a more accurate multipole (O_4, O_6, and/or VIP) magnetic field model with a current sheet. The developmental phase of this research was completed in this project while the implementational phase was only partially completed and will require additional research effort.

2.1 Non-Circular and Inclined Orbit of Europa

The orbit of Europa about Jupiter is time variable in nature. It is non-circular and non-elliptic with a Jovicentric distance that changes by ~0.18 R_J (Jupiter radii), is inclined to the planetary equator spin-plane by an angle that is ~0.5°, and has a perijove-apojove axis that undergoes a common coupled and nonuniform retrograde precession with Io. In an inertia frame, this retrograde precession rate, when averaged over a ten-year interval, has a value of about

$0.738°\ day^{-1}$ (i.e., a retrograde precession period of about 1.34 years), but it also exhibits time variability on a longer time scale. The location of Europa's orbit in the plasma torus, most importantly, the amplitude and local-time location of its orbital inclination relative to the plasma torus centrifugal equator plane, is important in determining the plasma torus properties at Europa and also in determining the lifetime history of neutral species in their circumplanetary trajectories near Europa's orbit. The accurate determination of Europa's orbit has been calculated at the Jet Propulsion Laboratory (JPL) by the Horizons Group (Jacobson 2001) from numerically integrating the equation of motions for the satellite that include multi-body gravitational interactions. These ephemeris calculations for Europa's orbit are contained in the Galilean satellite database that is part of the SPICE Toolkit available from JPL. We have therefore (1) acquired the SPICE Toolkit from JPL, (2) installed the SPICE Toolkit on AER computers, and (3) used the appropriate software libraries to calculate in Jovicentric coordinates the position and velocity of Europa in its orbit and to extract instantaneous information for its three-dimensional orbit about Jupiter. The numerical values for the orbit of Europa reported here are based upon the JPL JUP.204 ephemeris data file. The first attempt to express the orbit of Europa about Jupiter in terms of its six two-body orbital elements for an elliptical orbit proved to be too inaccurate for current purposes. The orbit of Europa about Jupiter is more complex, in particular because of the Laplace resonance between the satellites Ganymede, Europa, and Io. The spacetime nature of Europa's orbit has therefore been analyzed, and has also been successfully fitted with simple mathematical expressions that are valid for many orbital periods of the satellite about a selected absolute reference time. The parameters for these simple mathematical expressions are given later, in particular, for the time intervals that are appropriate for specifying the locations of Europa's orbit for the Galileo spacecraft's closest approach times.

2.1.1 Basic Spacetime Nature of Europa's Orbit

To understand the spacetime nature of the orbit of Europa about Jupiter, a more complete discussion of the mutual gravitational coupling between Io, Europa, and Ganymede is required. In this report, however, only a brief summary of information for Europa's orbit will be presented. A more complete discussion of the coupled nature of the noncircular orbits of Io and Europa is in preparation in a separate document.

The orbit of Europa is presented in a Jovicentric coordinate frame with the z-axis aligned along Jupiter's spin axis, the x-axis orientated so that the x-z plane contains the Sun-Jupiter line, and the y-axis completing the right-handed perpendicular frame. Introducing Jovicentric spherical coordinates (r, θ, ϕ) in this coordinate system by the transformation

$$x = r \cos\theta \sin\phi \tag{1a}$$
$$y = r \sin\theta \sin\phi \tag{1b}$$
$$z = r \cos\phi \tag{1c}$$

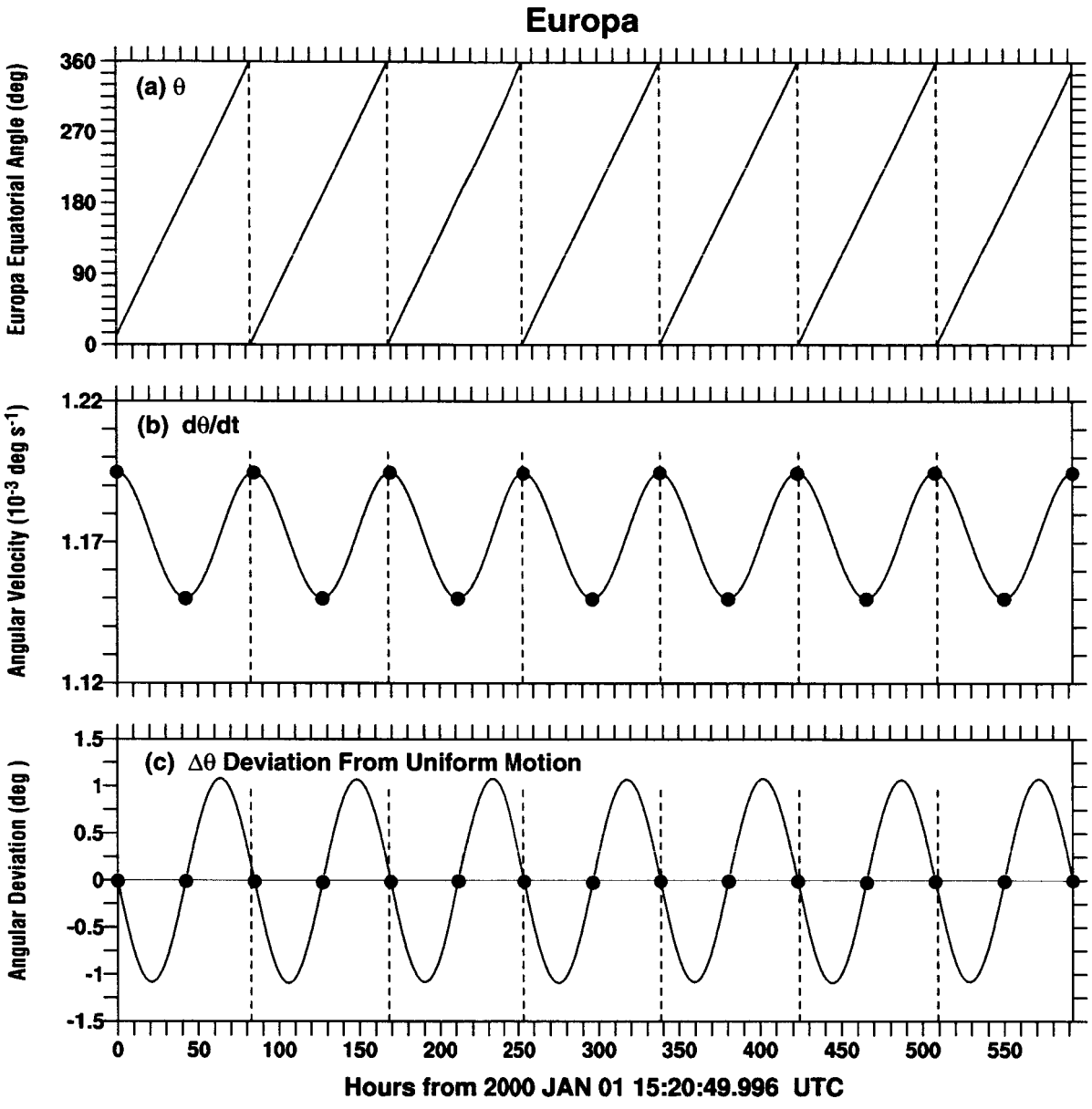

Figure 1. Orbital Angular Motion of Europa about Jupiter. The angular motion of Europa as determined from the ephemeris orbital calculations of the Horizons Group at the Jet Propulsion Laboratory is shown as a function of time for the indicated interval starting in January 2000. In (a), the solar longitude (equatorial orbit) angle θ of Europa is presented, where angular intervals of 360° about Jupiter in the Sun-orientated Jovicentric frame are indicated by the vertical dashed lines in the top, middle, and bottom panels. In (b), the time dependent equatorial angular velocity of Europa is shown, where the locations of Europa at perijove (blue dots) and apojove (red dots) are indicated in (b) and (c). In (c), the equatorial angular deviation Δθ of Europa's actual equatorial angle from its average equatorial angle predicted by its average equatorial angular velocity (1.172259×10^{-3} deg s^{-1}) over this time interval is shown.

the orbit of Europa is then determined by the radius, r, the solar longitude (i.e., equatorial orbit) angle, θ, where $\theta = 0°$ is in the x-z plane containing the Sun-Jupiter line, and the polar angle, ϕ.

The nature of the instantaneous angular motions of Europa about Jupiter is presented in Figure 1. In Figures 1a, the solar longitude angle θ of Europa about Jupiter is shown as a function of time. A completed 360° orbital period is indicated by the vertical dashed lines in all three panels of Figure 1. In Figure 1b, the angular velocity of Europa in the equatorial plane of Jupiter is shown. Europa's locations at perijove (blue dots) and apojove (red dots) are indicated in both the middle and lower panels. The angular velocity of Europa varies from periapse to apoapse about its average value by ~±1.9%. Note that as time increases, the blue and red dots slide to the left relative to the vertical dashed lines so that the time between successive perijove or apojove locations can be seen to occur in a shorter time interval than the period for Europa to complete one orbital trip around Jupiter. This is caused by the retrograde precession of the satellite perijove-apojove axis about Jupiter. In Figure 1c, the angular deviation of Europa from uniform angular motion based upon the satellites's actual average equatorial angular motion (i.e., a constant period) is shown. This means that by assuming a constant (but correctly-averaged period) for Europa's orbit, an error would be made in the actual equatorial angle θ of at most ~± 1.2° because of the nonuniform motion of the satellite in its orbits. The actual orbital equatorial period for Europa for the two-year time interval of 1990-1991 is, for example, very nearly constant, varying about its average value by only +0.026% to -0.015%.

The nature of Europa's motion in its orbits between successive apojoves and successive perijoves is presented for the month of January 1990 in Figure 2. In Figure 2a, the orbital radial period T_r, defined as the time interval between successive occurrences of the satellite at apojove (red) and between successive occurrences of the satellite at perijove (blue), is plotted with successive values connected by straight lines. The radial periods at apoapse and periapse undergo small fluctuations about a common average value but have different amplitude patterns. The amplitude of the fluctuation of the radial period for Europa is much larger at apoapse and varies there by ~±0.34%. Because of the retrograde precession of the perijove-apojove axis, the angular interval covered by the satellite between successive apojove or successive perijove angular locations is $2\pi - \Delta\psi$, where $\Delta\psi$ is the precession slippage angle. The precession slippage angles for Europa are plotted in Figure 2b with successive values at apoapse (red) and periapse (blue) connected by straight lines. The precession slippage angle can be seen to undergo small fluctuates about a common average value, but has a different behavior at apoapse and periapse. The amplitude of fluctuation of the precession slippage angle is larger at apoapse (~±38%) than at periapse (~±6%) and for the time interval shown varies from ~1.8 to 4.1°. The precession slippage angles at both apoapse and periapse are furthermore anti-correlated with their corresponding radial period in Figure 2a. The time-dependent retrograde angular precession rate defined by $\alpha = \Delta\psi / T_r$ is shown in Figure 2c and denoted at apoapse by α_a and at periapse by α_p. Because the

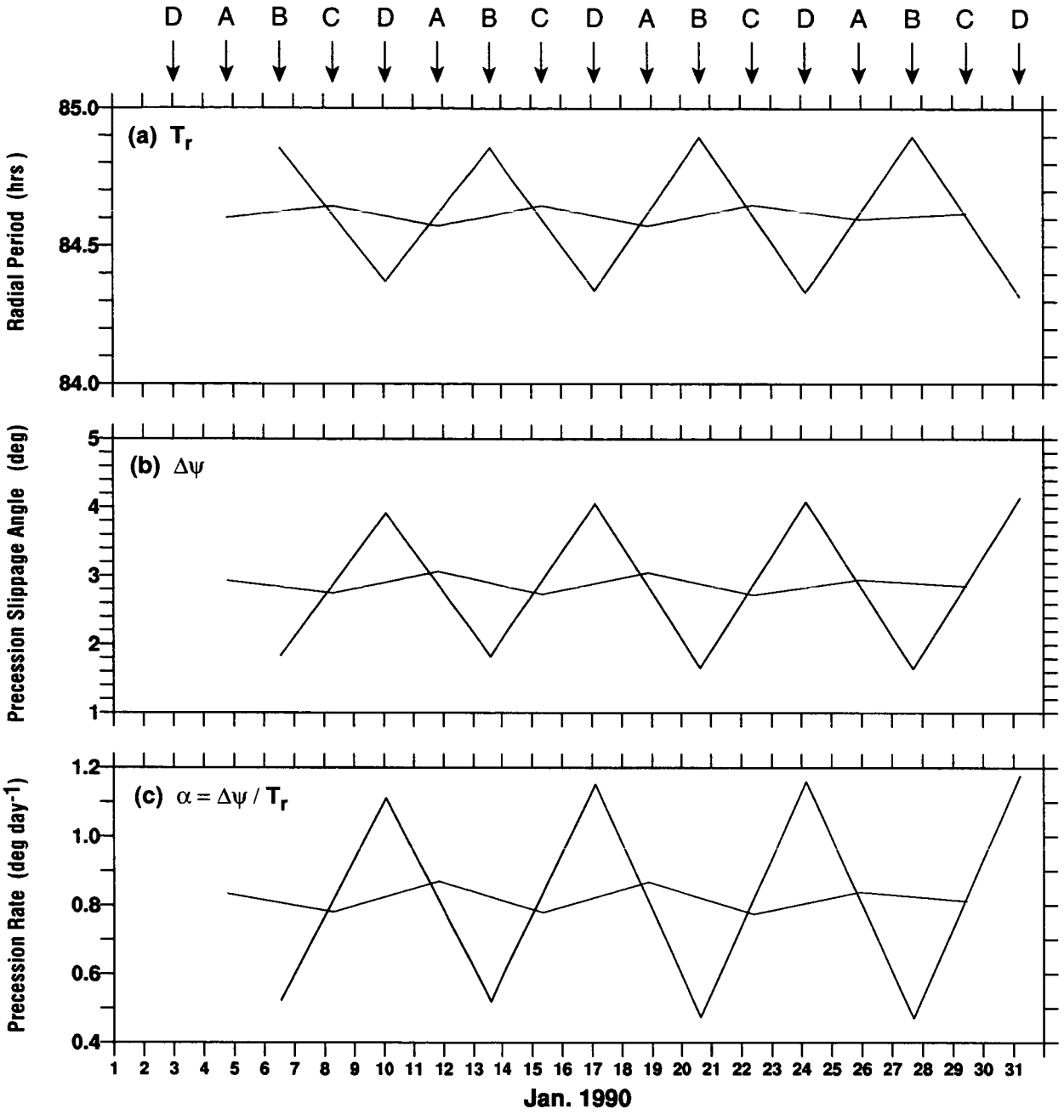

Figure 2. Retrograde Angular Precession and Period for the Perijove and Apojove of Europa's Orbit. In (a), Europa's radial period T_r between two successive apoapses (red) and between two successive periapses (blue) is plotted at the latter apse location and connected by straight lines. In (b), Europa's precession-slippage-angle, $\Delta\psi$, between two successive apojove (red) locations and between two successive periapse (blue) locations are plotted at the latter apse location and connected by straight lines. In (c), Europa's corresponding precession rate, $\alpha = \Delta\psi / T_r$, for the apoapse (red) and periapse (blue) points are plotted and connected by straight lines. The sets of times D, A, B, and C for Io at four successive occurrences of periapse are indicated. Orbit information is based upon 1 sec sampling of the JUP.204 ephemeris data file of the JPL Horizons Group.

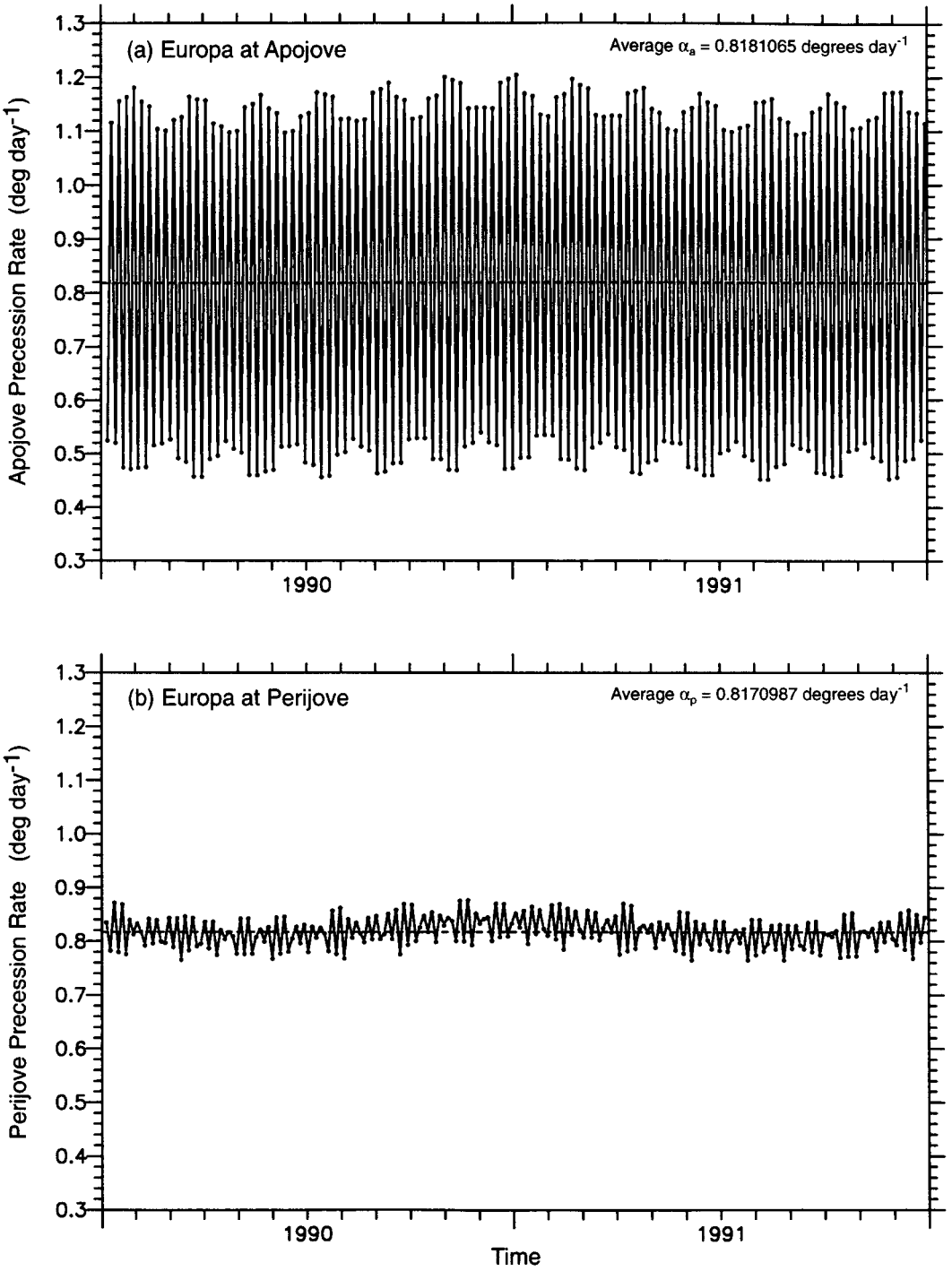

Figure 3. Angular Retrograde Precession Rate of Europa's Apojove and Perijove Positions. The retrograde angular precession rates about Jupiter of Europa's apojove position in (a) and perijove position in (b) are shown as a function of time in a Jovicentric coordinate frame with the z-axis aligned along Jupiter's spin axis and the x-axis orientated so that the x-z plane contains the Sun-Jupiter line. The precession rate is determined from the ephemeris orbital calculations of the Horizons Group at the Jet Propulsion Laboratory. The average precession rates shown by the black dashed lines are indicated. Orbit information is based upon 1 sec sampling of the JUP.204 ephemeris data file of the JPL Horizons Group.

variation in the value of T_r is slight compared to the variation in the value of $\Delta\Psi$, the values of α_a and α_p are correlated with the value of $\Delta\psi$. Since the values of $\Delta\psi$ and T_r are anticorrelated, their ratio values in α_a and α_p are accentuated with smaller values of $\Delta\psi$ forming even smaller ratios and with larger values of $\Delta\psi$ forming even larger ratios. The behavior of α_a and α_p over the two-year interval of 1990 and 1991 is shown for Europa in Figure 3. A longer-term variation for α_a and α_p with a period in excess of one year is evident. As indicated by the dashed lines in Figure 3, these behavior patterns produce slightly larger time-averaged values of α at apoapse than at periapse, which for this two-year interval are, respectively, $< \alpha_a > = 0.8181065^\circ$ day^{-1} and $< \alpha_p > = 0.8170987^\circ$ day^{-1}. The x-axis for the Sun-orientated Jovicentric coordinate (x,y,z) frame from which the solar longitude angle θ is measured, however, rotates once in an orbital period of Jupiter (11.86223 tropical years) in the opposite direction of the retrograde precession of the perijove-apojove axis and hence increases the rate from what its value would be determined in an inertial frame by an average amount of 0.083089°day^{-1}. Thus, these average retrograde precession rates for Europa of the perijove-apojove axis are reduced in an inertial frame to the value of $< \alpha_a >_{inertia} = 0.735018^\circ$ day^{-1} and $< \alpha_p >_{inertia} = 0.734010^\circ$ day^{-1}. For a longer ten-year time-average from 1990 to 2000, the slightly larger values of $< \alpha_a >_{inertia} = 0.7392235^\circ$ day^{-1} and $< \alpha_p >_{inertia} = 0.7382086^\circ$ day^{-1} are obtained, which are closer to the average value of 0.739507° day^{-1} given by Peale et al. (1979). Examination of the retrograde precession rates α_a and α_p over this ten-year time interval also indicates the existence of longer-term time dependent behavior so that these differences in the precession rates may be due to the effects of additional many-body gravitational forces that are included only in the numerically integrated solution.

The nature of Europa's radial orbital motion is presented in Figure 4 for the month of January 1990, where the time dependence of the solar longitude angle θ, the radial distance r, and the radial speed dr/dt are compared. Successive orbital periods of Europa about Jupiter determined in Figure 4a are indicated by the vertical dashed lines in all three panels. In Figure 4b, the orbital radial distance of Europa is seen to vary about its average value by $\sim\pm$ 0.09 R_J while in Figure 4c the radial speed of Europa is seen to vary about its average value by $\sim\pm$ 0.13 km s^{-1}. The location of the apoaspe point (red dot) and the periapse point (blue dot) of the orbit indicated in the lower two panels of Figure 4 can be seen to drift to the left relative to the satellite period (vertical dashed lines), as expected because of the retrograde precession rate of the periapse-apoapse axis. Examination of the maximum apoapse radial distance and the minimum periapse radial distance over a many-year time interval also shows that these apse radial distances also vary and have a period similar to the retrograde precession period.

The nature of Europa's motion in the vertical direction perpendicular to the equator spin plane of Jupiter is presented in Figure 5, where the time variations of the solar longitude angle θ, the vertical distance z, and vertical speed dz/dt are compared. As in Figure 4, the successive

orbital periods for the solar longitude angle of Europa about Jupiter are determined in Figure 5a and are indicated by the vertical dashed lines in all three panels. In Figure 5b, the orbital vertical

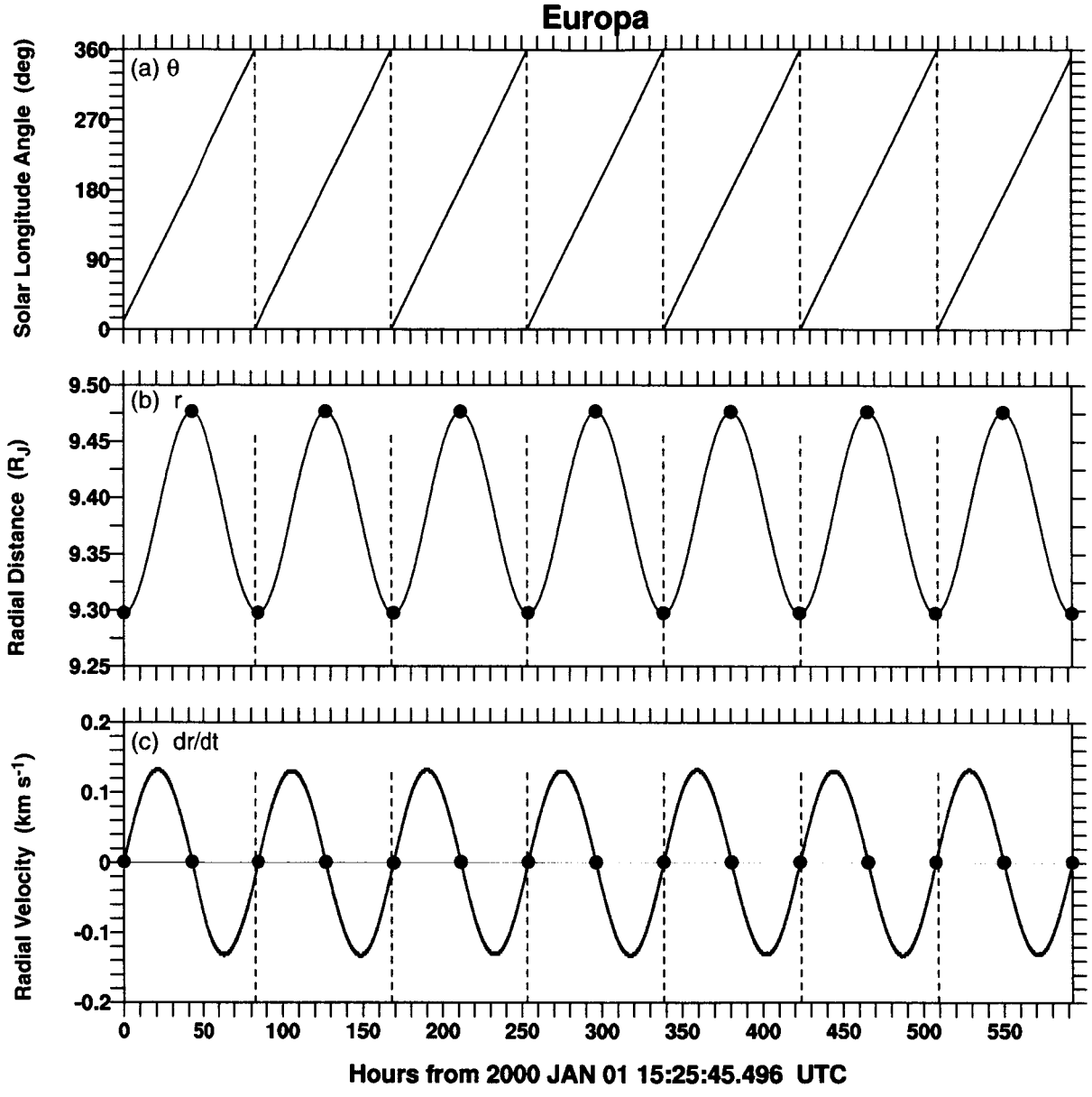

Figure 4. Orbital Radial Motion of Europa about Jupiter. The orbital radial motion of Europa as determined by the ephemeris orbital calculations of the Horizons Group at the Jet Propulsion Laboratory is shown for the indicated time interval in January 2000. In (a), the solar longitude angle of the satellite is presented, where angular intervals of 360° about Jupiter are indicated by the vertical dashed lines in the top, middle, and bottom panels. In (b), the orbital radial distance is shown, where in (b) and (c) the satellite locations at perijove (blue dots) and apojove (red dots) are indicated. In (c), the orbital radial speed is shown. Orbit information is based upon 1 sec sampling of the JUP.204 ephemeris data file of the JPL Horizons Group.

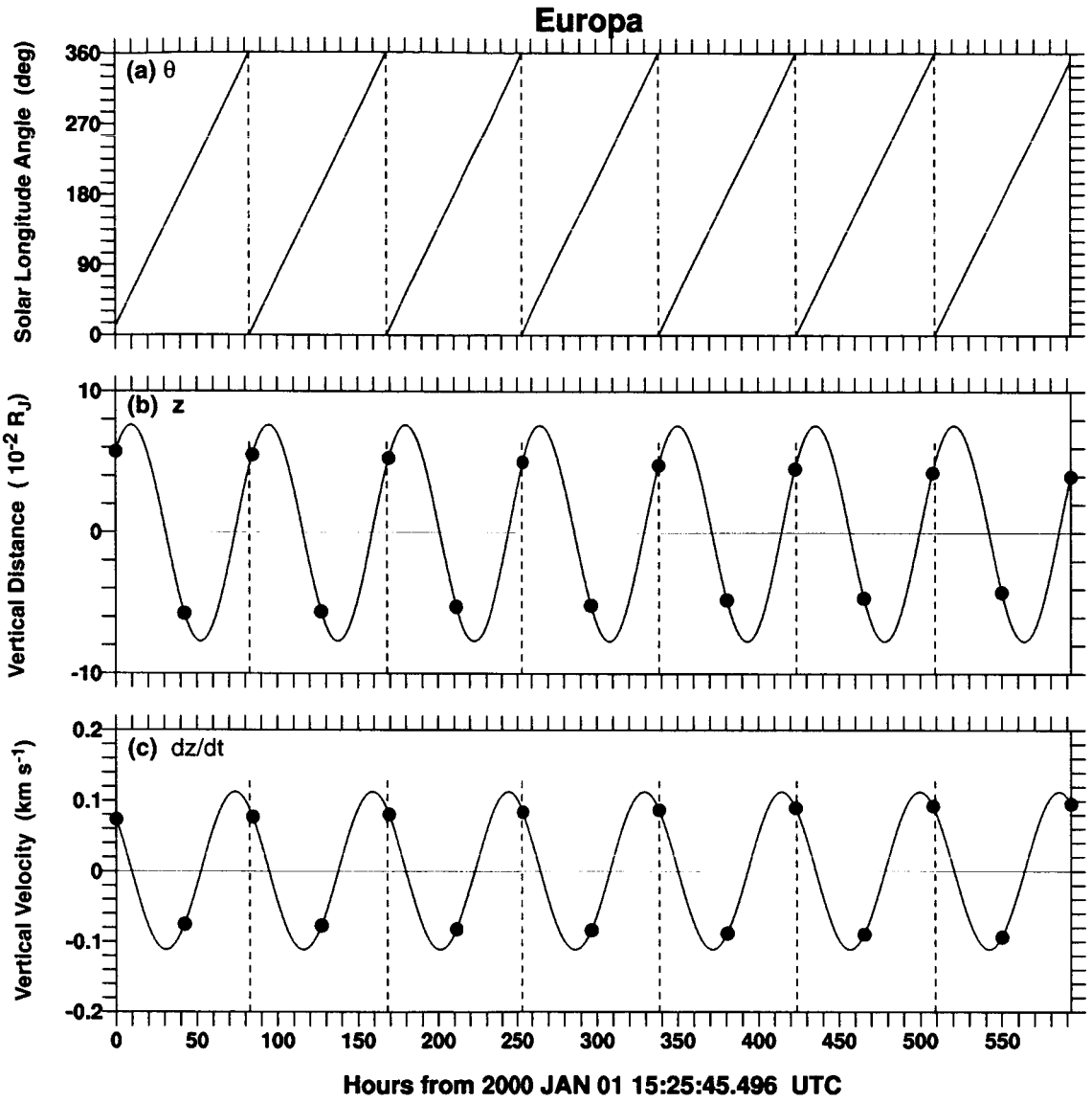

Figure 5. Orbital Vertical Motion of Europa about Jupiter. The orbital vertical motion perpendicular to the orbital spin plane of Jupiter of Europa as determined from the ephemeris orbital calculations of the Horizons Group at the Jet Propulsion Laboratory is shown for the indicated time interval starting in January 2000. In (a), the solar longitude angle of the satellite is presented, where angular intervals of 360° about Jupiter are indicated by the vertical dashed lines in the top, middle, and bottom panels. In (b), the orbital vertical distance is shown, where in (b) and (c) the satellite locations at perijove (blue dots) and apojove (red dots) are indicated. In (c), the orbital vertical speed is shown. Orbit information is based upon 10 sec sampling of the JUP.204 ephemeris data file of the JPL Horizons Group.

distance is seen to vary about its average value by ~± 0.08 R_J while in Figure 5c the vertical speed is seen to vary about its average value by ~± 0.11 km s^{-1}. The locations of apoaspe (red dot) and periapse (blue dot) points on the orbit are indicated in the lower two panels of Figure 5.

In Figure 5b, the vertical locations of the apoaspe and periapse points are seen to change in time and indicate that the vector orientation of the retrograde-moving periapse-apoapse axis is rotating in time relative to the maximum inclination vector of the satellite in its tilted orbit plane. In Figure 5c, the vertical velocity locations of the apoaspe and periapse points are seen to be located away from the locations of the maximum and minimum vertical velocities, because of the non-negligible inclination angle for Europa's orbit plane. This vertical orbital behavior in Figure 5 and the angular and radial orbital behaviors illustrated in Figures 1-4 indicate why, in general, three different average periods $\overline{T}_r$, $\overline{T}_\theta$, and $\overline{T}_\phi$ are required to approximately fit, over a relative short time interval, the radial, angular, and vertical positions of the satellite as a function of time.

2.1.2 Simple Mathematical Expressions for Europa's Orbit

A time-dependent approximate description for the orbit of Europa about Jupiter, valid for a limited time interval defined about an absolute specified reference time, may be prescribed in terms of simple fitted mathematical expressions. These fitted mathematical expressions in the Jovicentric spherical coordinates defined by Eq. (1) are given for the radial and angular locations of Europa's orbit (r_E, θ_E, ϕ_E) by

$$r_E = r_0 + \Delta r \sin\left[\frac{2\pi}{\overline{T}_r}(t - t_0) + \alpha_0^{(r)}\right] \tag{2a}$$

$$\theta_E = \text{Mod}\left[\left(\frac{2\pi}{\overline{T}_\theta}(t - t_0) + \theta_0\right),\ 2\pi\right] \tag{2b}$$

$$\phi_E = \frac{\pi}{2} + \Delta\phi \sin\left[\frac{2\pi}{\overline{T}_\phi}(t - t_0) + \alpha_0^{(\phi)}\right] \tag{2c}$$

where t_0 is a specified reference time. For a selected number of satellite periods in the vicinity of an absolute time t, the radial amplitude variation Δr is determined by the average maximum and minimum excursion of Europa's numerically calculated radius from its mean value r_0, the average radial orbital period $\overline{T}_r$ is determined by the average time separation between the numerically calculated maximum and minimum values of the radius r, and the radial phase angle $\alpha_0^{(r)}$ is determined so as to obtain the minimum least-square error between the function r_E and the numerically calculated r values over the selected number of satellite periods. For a selected number of satellite periods in the vicinity of an absolute time t, the average solar longitude (equatorial orbit) period $\overline{T}_\theta$ is determined by the average time separation between the 2π periodic behavior of θ, and the equatorial phase angle θ_0 is determined so as to obtain the minimum least-square error between the function θ_E and the numerically calculated θ values

Table 1. Europa's Orbital Location at the Galileo Spacecraft's Closest Approach Times

	UTC	ET	r	ϕ	θ
E4	1996 DEC 19 06:52:58.000	$-9.574955.981643\times10^{7}$	9.453634	90.20862	70.46082
E6	1997 FEB 20 17:06:10.000	$-9.026956781476\times10^{7}$	9.457247	90.43707	14.82751
E11	1997 NOV 06 20:31:44.000	$-6.787963281740\times10^{7}$	9.319544	90.43921	344.1226
E12	1997 DEC 16 12:03:20.000	$-6.445413681651\times10^{7}$	9.441667	90.11095	39.96433
E14	1998 MAR 29 13:21:05.000	$-5.555027181435\times10^{7}$	9.461577	90.04206	36.48459
E15	1998 MAY 31 21:12:56.000	$-5.007876081509\times10^{7}$	9.470866	90.40883	330.7864
E16	1998 JUL 21 05:03:45.000	$-4.573051181645\times10^{7}$	9.346196	89.99971	27.44830
E17	1998 SEP 26 03:54:20.000	$-3.994587681764\times10^{7}$	9.350306	90.35428	328.5189
E18	1998 NOV 22 11:44:56.000	$-3.499284081711\times10^{7}$	9.308216	89.96776	16.27665
E19	1999 FEB 01 02:19:50.000	$-2.889234581521\times10^{7}$	9.317445	90.26906	327.8417
E26	2000 JAN 03 17:59:43.000	$1.944471839925\times10^{5}$	9.459488	90.46304	223.7394

Note: UTC is calendar date and UT time of closest approach; ET is time of closest approach expressed as seconds from noon on Jan. 1, 2000 UT; r is radial distance from Jupiter in units of R_J (= 71,492.0 km); ϕ is the inclination relative to Jupiter's equatorial plane in degrees, with 90° representing the equatorial plane; θ is the solar phase angle in degrees, with 0° pointing towards the Sun.

Table 2. Europa's Orbital Fit Parameters as Determined from JPL JUP.204 Ephemeris Data

	E4	E6	E11	E12	E14	E15	E16	E17	E18	E19	E26
r_0	9.38743	9.38747	9.38639	9.38727	9.38748	9.38758	9.38669	9.38669	9.38634	9.38637	9.38748
Δr	0.0883428	0.0886631	0.0873790	0.0872508	0.0879386	0.0886343	0.0890051	0.0890354	0.0884650	0.0874335	0.0895807
α_r	4.8845	4.8924	4.9234	4.9325	4.9574	4.9672	4.9715	4.9735	4.9754	4.9844	5.0443
$\overline{T}_r$	*84.618*	*84.618*	*84.61819*	*84.618*	*84.618*	*84.618*	*84.618*	*84.618*	*84.618*	*84.618*	*84.618*
$\Delta\phi$	0.451049	0.451580	0.454986	0.454297	0.456218	0.458696	0.458790	0.458096	0.459579	0.462676	0.467254
α_ϕ	0.93455	1.4902	2.8831	3.6808	3.6080	1.6111	0.88765	4.0458	4.1048	4.7483	0.29993
$\overline{T}_\phi$	84.861	85.648	84.722	84.398	84.491	85.093	85.694	86.111	86.065	85.509	84.491
θ_0	148.135	170.054	156.078	167.533	151.274	215.045	178.819	142.104	180.677	139.553	137.220
$\overline{T}_\theta$	85.247	85.297	85.281	85.295	85.281	85.342	85.308	85.278	85.308	85.278	85.283

Note: r_0 and Δr in R_J (= 71,492.0 km); $\overline{T}_r$, $\overline{T}_\phi$, and $\overline{T}_\theta$ in hours; α_r and α_ϕ in radians; $\Delta\phi$ and θ_0 in degrees; t_0= 1995 DEC 02 10:23:53.172 (= $-1.288281056449\times10^8$ seconds from noon on Jan. 1, 2000 UT).

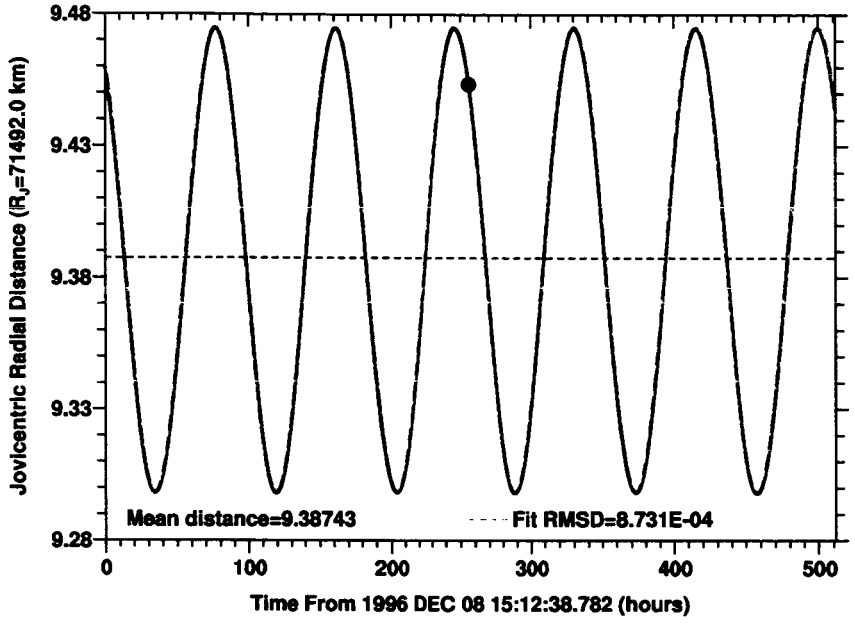

Figure 6. Radial Distance of Europa from Jupiter for the E4 Galileo Spacecraft Encounter. The time variation of the Jovicentric radial distance of Europa centered on the E4 Galileo spacecraft encounter (blue dot) is shown as a function of time by the solid red line as determined from the numerical orbit calculation and by the green dashed line as determined from the fitted mathematical expression (2a). The mean radial distance r_0 is indicated by the horizontal dashed line.

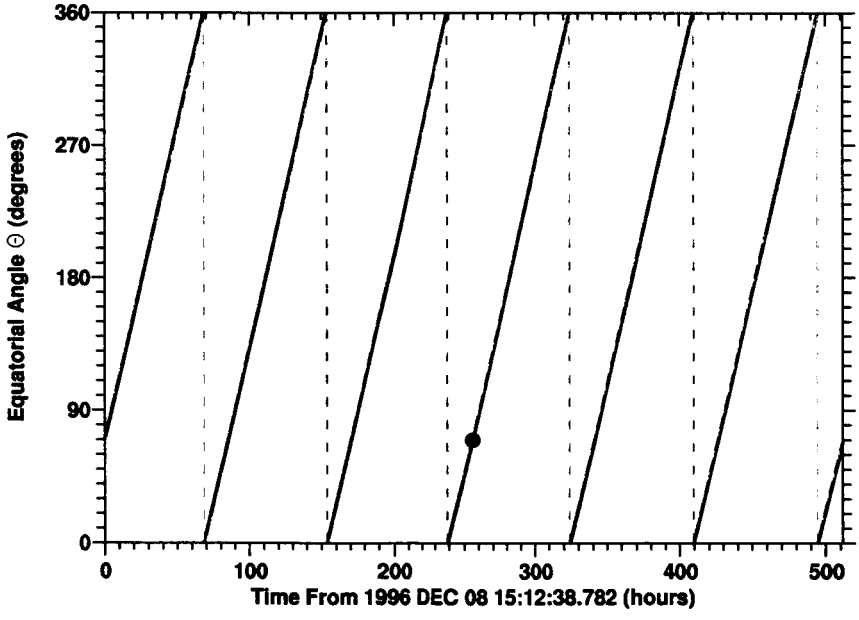

Figure 7. Equatorial Angle of Europa in Jupiter's Equator Plane for the E4 Galileo Spacecraft Encounter. The time variation of the equatorial angle of Europa centered on the E4 Galileo spacecraft encounter (blue dot) is shown as a function of time by the red line as determined from the numerical orbit calculation and by the green dashed line as determined by the fitted mathematical expression (2b). The vertical dashed lines separate each 360° of orbital motion.

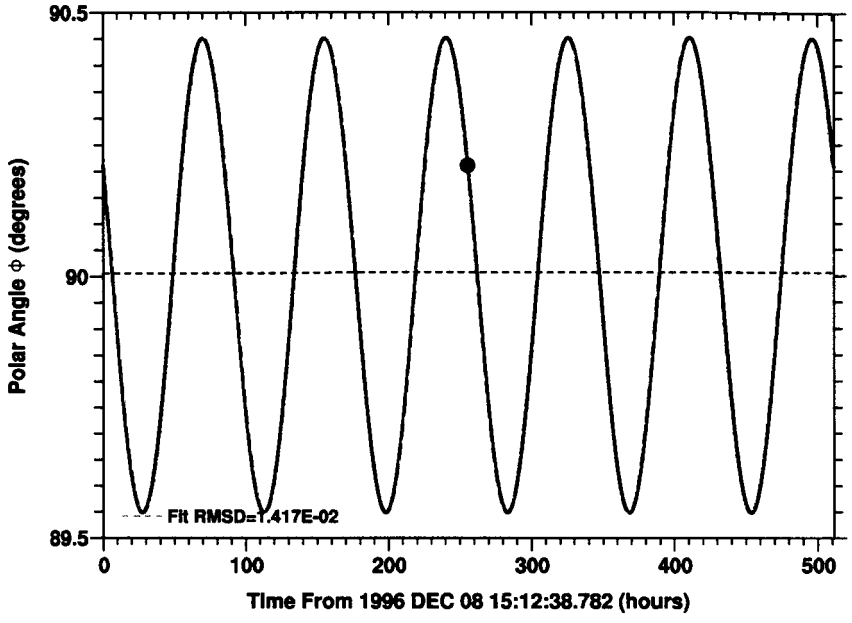

Figure 8. Polar Angle of Europa from Jupiter's Spin Axis for the E4 Galileo Spacecraft Encounter. The time variation of the polar angle of Europa centered on the E4 Galileo spacecraft encounter (blue dot) is shown as a function of time by the solid red line as determined from the numerical orbit calculation and by the green dashed line as determined from the fitted mathematical expression (2b). The mean polar angle, indicated by the horizontal dashed line, is very close to 90°.

over the selected number of satellite periods. For a selected number of satellite periods in the vicinity of an absolute time t, the polar-angle amplitude variation $\Delta\phi$ is determined by the average maximum and minimum angular excursion of Europa's numerically calculated ϕ value from $\pi/2$, the average polar orbital period $\overline{T}_\phi$ is determined by the average time separation between the numerically calculated maximum and minimum values of ϕ , and the polar phase-angle $\alpha_0^{(\phi)}$ is determined so as to obtain the minimum least-square error between the function ϕ_E and the numerically calculated ϕ values over the selected number of satellite periods.

The closest approach times and the corresponding orbital positions (r, θ, ϕ) of Europa for its eleven encounters with the Galileo spacecraft are presented in Table 1. The values for the nine parameters in the Eq. (2) appropriate for times near these eleven encounter events are presented in Table 2. The excellent agreement of the fitted mathematical expressions in Eq. (2) and the numerically calculated values for (r_E, θ_E, ϕ_E) is illustrated in Figures 6, 7, and 8 for six satellite orbital periods centered on the absolute time for the E4 encounter of the Galileo spacecraft with Europa. In Figure 6, the time variability of the Jovicentric radial distance about its mean location (dashed horizontal line) is shown by the red solid curve as calculated numerically and is very well fitted by the expression in Eq. (2a) shown by the green dashed line. In Figure 7, the angular motion of Europa's orbit about Jupiter is shown by the red solid curve as calculated numerically and is very well fitted by the expression in Eqs. (2b) shown by the green

dashed line. In Figure 8, the time dependent inclination of Europa's orbit relative to the equator plane of Jupiter is shown in terms of Europa's polar angle by the red solid curve as calculated numerically and is very well fitted by the expression in Eqs. (2c) shown by the green dashed line. The maximum inclination in Figure 8 and in Table 2 is a little less than 0.5°. Similar excellent fits for the location of Europa in its orbit about Jupiter are also obtained by using the expressions in Eqs. (2) and the parameters in Table 2 for times centered about the remaining ten Galileo spacecraft encounter events in Table 1.

In Table 1, values for the average radius r_0 of Europa's orbit vary slightly from 9.38634 to 9.38758 R_J and are very similar to the nominal value for Europa's semi-major axis. The values for the average equatorial-angle period $\overline{T}_\theta$ of Europa's orbit also varies slightly from 85.247 to 85.342 hrs and are very similar to the nominal value for Europa's orbit period. The average radial period for maximum and minimum radial excursion $\overline{T}_r$ = 84.618 hrs is the same for all of the encounter fits but is always smaller than the average equatorial-angle period $\overline{T}_\theta$ for Europa's orbit by a significant amount that for these nine encounters varies between 0.629 to 0.724 hrs. Finally, in Table 2, the average period for maximum z-excursion $\overline{T}_\phi$ is sometimes smaller and sometimes larger than the average equatorial-angle period $\overline{T}_\theta$ of Europa's orbit. An analysis over a more continuous time-base than that included in Table 2 is required to determine an average apojove-perijove axis period and to determine if there is a secular drift in $\overline{T}_\phi$ relative to $\overline{T}_\theta$. Thus in summary, the three different spatial motions of Europa's orbit are forced at slightly different angular frequencies because of multi-body gravitational effects and can all be accurately represented for a limited time interval about a prescribed reference time t by the simple expressions in Eq. (2).

2.2 Improvement in the Plasma Torus Structure and Properties near Europa's Orbit

The current description of the structure of the corotating plasma torus in the neutral cloud model is based upon an offset-tilted planetary dipole magnetic field, an east-west electric field, and plasma torus properties that were determined at the time of the encounter of the Voyager 1 spacecraft with Jupiter. For radial distances beyond about 8 Jupiter radii (Europa's orbit is at 9.38 R_J), as noted by Bagenal (1994), the projection of the electron and ion densities from values measured at the Voyager spacecraft location to values in the plasma torus centrifugal equator will be dependent upon the magnetic field model adopted, since the spacecraft was well below the symmetry plane. The current plasma torus electron density as determined by a dipole magnetic field projection of Voyager data in the neutral cloud model is ~70 cm^{-3} at Europa's orbit (similar to Bagenal's dipole value), but different than using O_4 or O_6 magnetic field model projections with current sheets, giving electron densities as large as ~160 cm^{-3}. Efforts have therefore been under way to improve the plasma properties near Europa for a magnetic field description by incorporating the effects of the more accurate magnetic projection (with a current sheet), which has been previously developed for our in-house empirical Io plasma torus models

(Woodward and Smyth 1994), and also to update, when available, the plasma torus properties using the GEM measurements acquired during the Europa passes. Unfortunately, a description of the plasma torus for the GEM measurements has not been forthcoming to date due to a number of technical reduction difficulties and data deficiencies that have not been overcome by the scientific community. Consequently, the best description of the plasma torus still remains that determined for the Voyager 1 spacecraft flyby of Jupiter in 1979 (Bagenal 1994), a version of which is already included in the neutral cloud models. Additional efforts were, therefore, expended to update in the earlier empirical Io plasma torus models of Woodward and Smyth (1994) the more recent improvements in the magnetic field configuration. These improvements have recently been completed in this project, but this new plasma torus description has yet to be incorporated in the neutral cloud model.

III. PLASMA TORUS CHEMISTRY

To undertake Europagenic plasma source studies, appropriate new plasma chemistry for the lifetime of the new neutral species H_2, O_2, and H_2O in the inner magnetosphere must be incorporated in the neutral cloud models. Based upon plasma properties determined by the PLS instrument of the Voyager 1 spacecraft, the total (electron impact ionization and charge exchange) lifetimes of the molecular species O_2, H_2 and H_2O as well as several atomic species are largely dominated in and near the plasma torus symmetry plane by electron impact ionization because the electron temperature at Europa's orbit is ~20 eV and is much larger than the energy thresholds for the reactions. Implementation in the neutral cloud model of the dominant chemistry for photo and electron impact reactions given in Table 3 has been completed in this project as well as the addition of important ion charge exchange reactions. The rates given in Table 3 are for nominal plasma torus properties at Europa's orbit while the plasma torus properties in the neutral cloud models are three-dimensional and local-time dependent. A comparison in Table 3 of the electron and photo rates for the same molecular dissociative reaction branch shows that electron processes in the plasma torus at Europa's orbit are much more important than photo processes.

In Europa's atmosphere, to first order, the same electron dissociation rates shown in Table 3 will apply since the Alfvénic electrodynamic interaction is incompressible in nature. Many of the electron and photo dissociation reactions in Table 3 are known to be exothermic with excess energies of ~1 to a few eV so that the product species O and H indicated in red are kinetically hot, having significantly-nonthermal initial velocities. The light H atoms will have velocities large compared to Europa's gravitational escape speed, will not be significantly thermalized in collisions with the heavy O_2 molecules in Europa's atmosphere, will hence easily escape the gravitational grasp of the satellite with significant velocities, and will therefore populate a large spatial volume in the circumplanetary space. The heavier O atoms will have velocities more comparable to Europa's gravitational escape speed, will be somewhat

Table 3. Reaction Rates for H_2, O_2 and H_2O at Eurora's Orbit		
Reaction	**Rate (s^{-1})**	**Reference**
H_2 + hν -> H + H	3.1–7.1 x 10^{-9}	Huebner et al. 1992
H_2 + hν -> H_2^+ + e	2.0–4.2 x 10^{-9}	Huebner et al. 1992
H_2 + hν -> H + H^+ + e	0.35–1.0 x 10^{-9}	Huebner et al. 1992
H_2 + e -> H + H + e	3.7 x 10^{-7}	Dalgarno et al. 1999; Stibbe and Tennyson 1999
H_2 + e -> H_2^+ + 2e	7.7 x 10^{-7}	Straub et al. 1996
H_2 + e -> H + H^+ + 2e	4.0 x 10^{-8}	Straub et al. 1996
O_2 + hν -> O + O	1.6–2.5 x 10^{-7}	Huebner et al. 1992
O_2 + hν -> O_2^+ + e	1.7–4.4 x 10^{-7}	Huebner et al. 1992
O_2 + hν -> O + O^+ + e	0.41–1.3 x 10^{-8}	Huebner et al. 1992
O_2 + e -> O + O	9.7 x 10^{-7}	Wakiya 1978; Garret et al. 1985
O_2 + e -> O_2^+ + 2e	1.2 x 10^{-6}	Krishnakumar & Srivastava 1992
O_2 + e -> O + O^+ + 2e	1.66 x 10^{-6}	Krishnakumar & Srivastava 1992
H_2O + hν -> H + OH	3.8–6.5 x 10^{-7}	Huebner et al. 1992
H_2O + hν -> H_2 + O (^1D)	2.2–5.5 x 10^{-8}	Huebner et al. 1992
H_2O + hν -> H + H + O	2.8–7.1 x 10^{-7}	Huebner et al. 1992
H_2O + hν -> H_2O^+ + e	1.2–3.1 x 10^{-8}	Huebner et al. 1992
H_2O + hν -> OH^+ + H + e	2.1–5.6 x 10^{-9}	Huebner et al. 1992
H_2O + hν -> OH + H^+ + e	0.48–1.5 x 10^{-9}	Huebner et al. 1992
H_2O + hν -> H_2 + O^+ + e	2.2–8.2 x 10^{-10}	Huebner et al. 1992
H_2O + e -> H + OH	7.2 x 10^{-6}	1/2 of SO_2 dissociation rate
H_2O + e -> H_2O^+ + 2e	1.1 x 10^{-6}	Shirai et al. 2001
H_2O + e -> OH^+ + H + 2e	2.1 x 10^{-7}	Shirai et al. 2001
H_2O + e -> OH + H^+ + 2e	1.8 x 10^{-7}	Shirai et al. 2001
H_2O + e -> H_2 + O^+ + 2e	1.5 x 10^{-8}	Shirai et al. 2001
H_2O + e -> H_2^+ + O + 2e	1.2 x 10^{-9}	Shirai et al. 2001

Assumed plasma properties: core electron density = 38 cm^{-3} (120 cm^{-3}), core electron temperature = 20 eV, suprathermal electron density = 2 cm^{-3}, suprathermal electron temperature = 250 eV; low (high) proto-dissociation rates are for the quiet (active) Sun.

thermalized in collisions with the heavy O_2 molecules in Europa's atmosphere, will hence escape the gravitational grasp of the satellite with small velocities, and will therefore occupy a spatial volume that is much more space confined in the vicinity of Europa's orbit. The light species H_2 is also expected to escape the atmosphere with smaller velocities and will therefore also be more space confined in the vicinity of Europa's orbit. The sputtered loss of O_2 from Europa's atmosphere by torus ions and ionospheric O_2^+ ions with their slowed electrodymanic velocities of

~20 km s^{-1} is expected, for the most part, to produce very fast O by dissociative knock-on collisions and fast O_2 by charge exchange collisions. These fast O and O_2 species will rapidly depart from Europa's orbit, will escape from the Jupiter's gravity, and will form large O and O_2 zenocoronae about the planet. In addition, Europa's atmosphere is expected to lose some O_2 by direct ion loss primarily in the form of O_2^+ pickup ions. The primary species that are expected to escape Europa and form neutral clouds near its orbit are therefore O and H_2.

IV. NEUTRAL CLOUDS AND PICKUP ION PRODUCTION RATES

4.1 Europa's Atmosphere

The presence of water ice on Europa and the liberation of material from the surface by the radiolysis of the ice by magnetospheric energetic ion and electrons and by photolysis is thought to be the primary mechanism that gives rise to an atmosphere dominated by the non-condensable species O_2 and a much smaller population of the non-condensable species H_2. The existence of an O_2 atmosphere with a column density of ~0.24-1.4 x 10^{15} cm^{-2} was determined from the analysis of HST observations of atomic oxygen ultraviolet emissions produced by electron impact dissociative excitation of O_2 (Hall et al. 1998, 1995). From kinetic theory modeling studies for the atmosphere, the heavy species O_2 is expected to be concentrated primarily at low altitudes with the much lighter species H_2 becoming the dominant species at higher altitudes. The atmospheric supply rate of O_2 liberated from the surface is uncertain, but the most recent estimates (Johnson et al. 2004; Shematovich et al. 2004) suggest values of ~2-6 x 10^9 molecules cm^{-2} s^{-1}, which corresponds to a total isotropic source rate from the satellite of ~0.6-1.8 x 10^{27} molecules s^{-1}. The atmospheric supply rate of H_2O from the surface is uncertain but is likely comparable (Shematovich et al. 2004). Unless, however, the initially liberated velocity distribution of H_2O contains a nonthermal component that escapes directly from Europa's thin atmosphere, the non-escaping H_2O will condense rapidly on the surface and, consequently, becomes a very minor and otherwise unimportant species in the atmosphere. The atmospheric supply rate of H_2 from the surface is also uncertain but is likely to be about a factor of two larger than that for O_2.

To maintain a steady state atmosphere, the net surface supply rate of O_2 and H_2 to the atmosphere must gravitationally escape from Europa and will populate for lower velocities the neutral clouds near the satellite's orbit and will populate for higher velocities the zenocorona extending in the circumplanetary environment to large (100's to 1000's R_J) radial distances from Jupiter. The major escape mechanisms for the atmosphere were recently estimated by Saur et al. (1998) in their investigation of the electrodynamic interaction of the planetary magnetospheric plasma with Europa. They determined an escape rate of 8.5 x 10^{26} molecules s^{-1} that was produced primarily (86%) by atmospheric sputtering of O_2 and secondarily (14%) by loss of O_2^+ pickup-ion loss produced by electron impact ionization. Their atmospheric sputtering escape rate was based upon the interaction of plasma torus ions and the much more abundant O_2^+

ionospheric ions (which are created and slowed in the electrodynamic interaction to ~20 km s^{-1}) for the processes of (a) knock-on collisions with O_2, which primarily produce O + O*, where O* is a fast atom that rapidly escapes the Jupiter system, and (b) charge exchange with O_2 which produces fast O_2 that also rapidly escapes the Jupiter system. In addition to O_2, the net atmospheric surface supply rate of relatively light species H_2 is expected to readily escape from Europa's atmosphere with an escape rate ~1-2 x10^{27} molecules s^{-1} (i.e., roughly estimated to be twice that for O_2). The estimates of Saur et al. (1998) are based upon a single species O_2 atmosphere that is devoid of dissociative atmospheric chemistry. The inclusion of atmospheric chemistry for electron impact and photo-dissociation of O_2 and H_2 with non-thermal exothermic O and H products will provide additional avenues for neutral escape. The escape of non-thermal exothermic O created by photodissociation of O_2 was considered by Shematovich and Johnson (2001) and Shematovich et al. (2004) with an estimated escape rate of ~1 x 10^{26} O atoms s^{-1}. Since they neglected the dominant source of non-thermal exothermic O created by electron impact dissociation of O_2, which is a factor of ~4 to 6 times larger in Table 3, a rough estimate of the escape rates of O is ~5 x 10^{26} atoms s^{-1}.

4.2 Neutral Clouds of Europa

Preliminary model calculations for the neutral cloud formed about Jupiter by the escape of O atoms from Europa have therefore been undertaken for an adopted satellite isotropic escape source rate of 5 x 10^{26} atoms s^{-1} and for a simple characteristic monoenergetic initial speed of 2.5 km s^{-1} ejected from an adopted satellite exobase radius of 1569 km (surface) where the escape speed is 2.02 km s^{-1}. The two-dimensional distribution of the O column density viewed perpendicular to the satellite orbit is shown in Figure 9. The O column density is highly peaked about Europa's position, is enhanced in the forward cloud (ahead of the satellite) confined largely between Io's and Europa's orbits, and extends at a value larger than 1 x 10^{10} atoms cm^{-2} all around Jupiter. In Figure 10, model calculations for the radial profiles of the longitudinally-averaged column density for Europa's neutral O cloud corresponding to Figure 9 and for Europa's H_2 neutral cloud with a source rate of 2 x 10^{27} molecules s^{-1} and a monoenergetic initial ejection speed of 2.5 km s^{-1} are compared to Io's O and S neutral clouds as determined recently by Smyth and Marconi (2003). The total cloud population for Europa's O neutral cloud (in red) of 4.0 x 10^{32} atoms is comparable to Io's S cloud of 3.1 x 10^{32} atoms (in black) but is smaller than Io's O neutral cloud (in black) of 1.2 x 10^{33} atoms. The total cloud population for Europa's H_2 neutral cloud (in green) of 2.0 x 10^{33} molecules is larger than the population of Io's O and S clouds. Mauk et al. (2003) recently suggested that a neutral population for Europa's H neutral cloud of ~4.5–9 x 10^{33} atoms would be required to produced ENA detected by measurements from the Cassini spacecraft. Note that the average radial profile for the column density of Europa's neutral H_2 cloud exceeds that for Io's O and S clouds at a radial distance of ~7.5 R_J and should introduce new plasma-neutral interactions beyond that boundary.

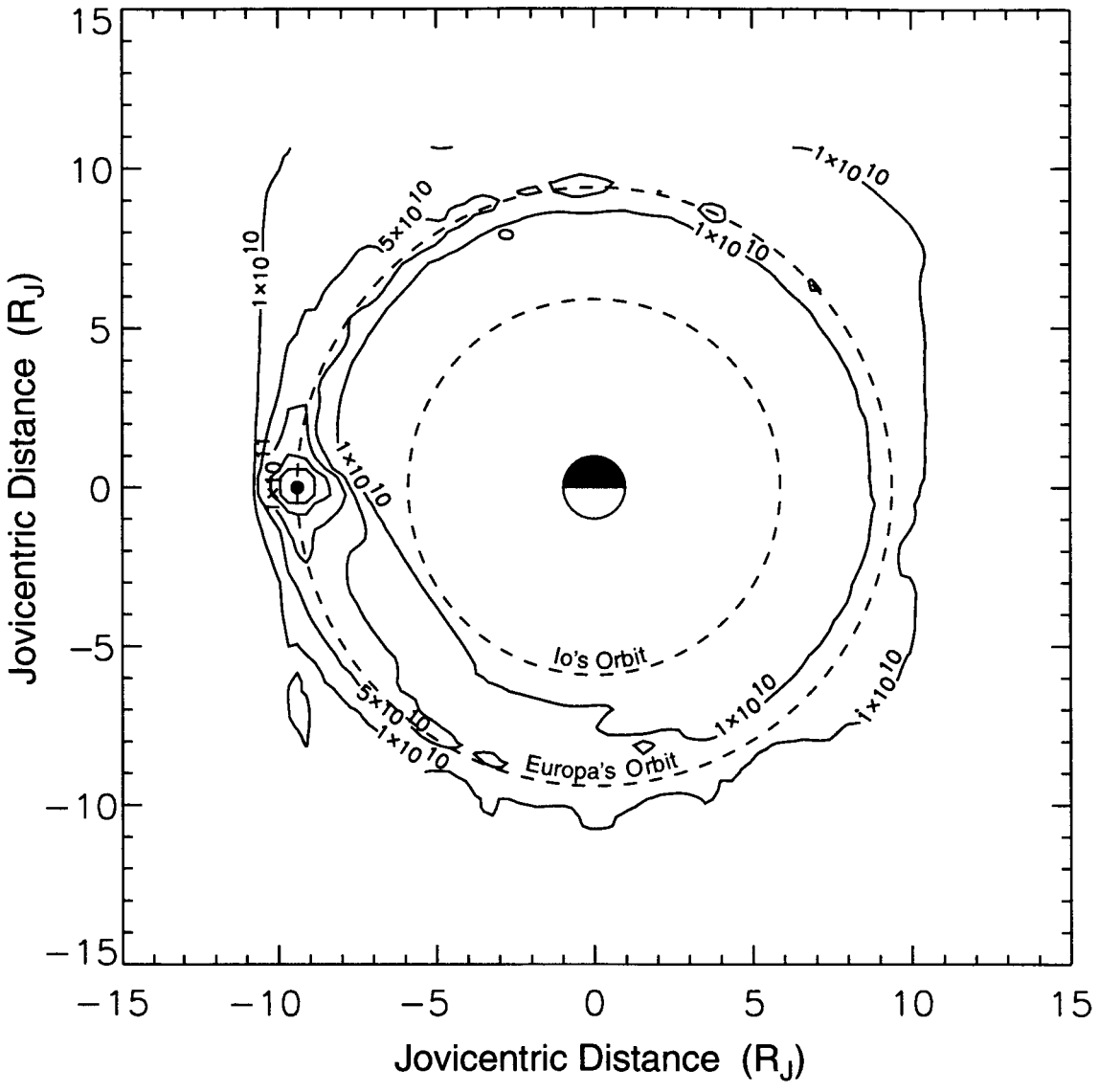

Figure 9. Europa's Circumplanetary Distribution of Atomic Oxygen. A model calculation for the O column density (units of atoms cm^{-2}) of Europa's neutral cloud is shown as viewed perpendicular to the satellite orbit plane. An isotropic source rate of 5 x 10^{26} atoms s^{-1} ejected from an adopted satellite's exobase radius of 1569 km with a simple monoenergetic speed of 2.5 km s^{-1} is assumed. The orbits of Io and Europa (dashed circles) and Europa's location (dot) on its orbit are shown. The unmarked contours about Europa, from outside to inside, are 2.x 10^{11} and 4 x 10^{11} atoms cm^{-2}.

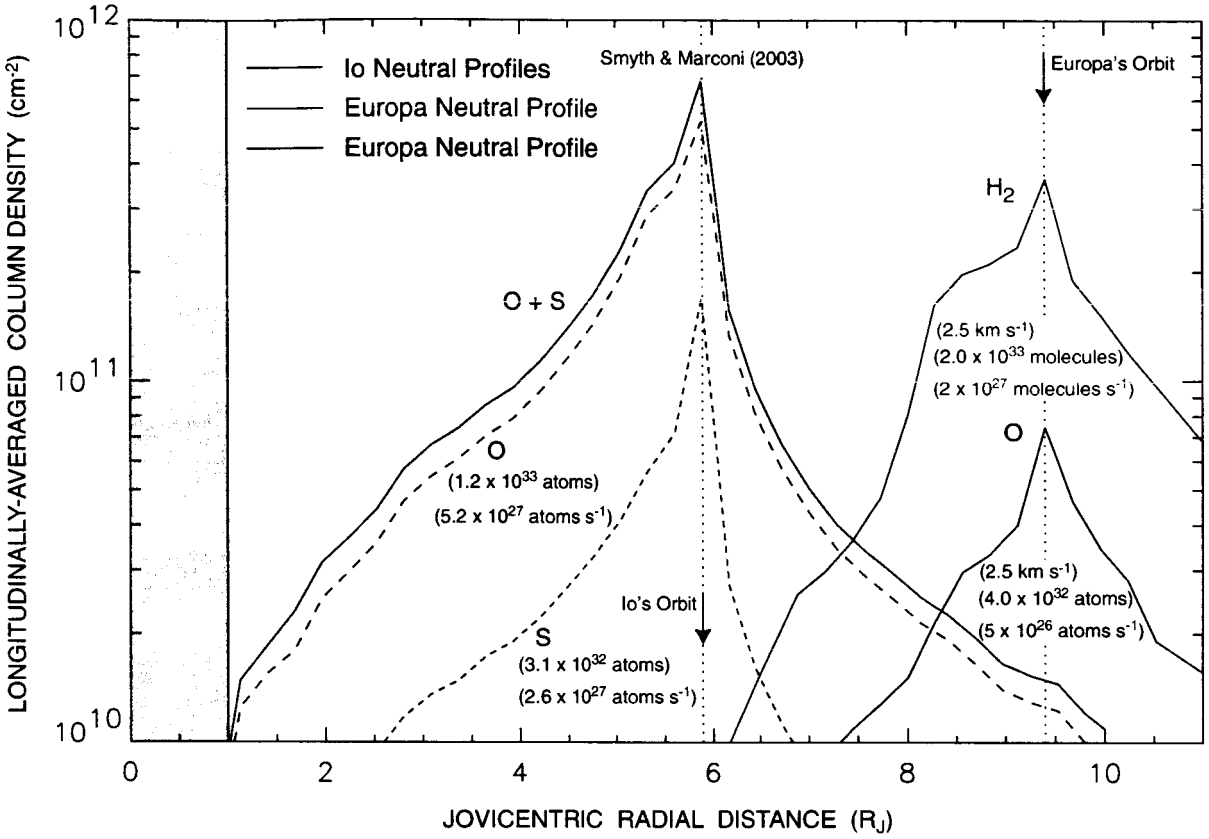

Figure 10. Average Radial Neutral Column Density Profiles for Io's and Europa's Neutral Clouds. The model calculated longitudinally-averaged column density profiles are shown for Io's neutral O, S, and O+S clouds from Smyth and Marconi (2003) in black, for Europa's O clouds calculated in this project in blue, for Europa's H cloud calculated earlier in this project in green, and for the Europa's H cloud scaled earlier in this project to the cloud population of Mauk et al. (2003) in red. The neutral cloud atom source rates and total cloud populations are indicated.

4.3 Europa's Ion Production Rates for the Planetary Magnetosphere

The circumplanetary distribution for the instantaneous total O^+ production rate integrated along the magnetic field lines that is created by Europa's O neutral cloud in Figure 9 because of electron impact (EI) and charge exchange (CE) processes in the plasma torus is shown in Figure 11. The two-dimensional instantaneous ion production rate is, as expected from the neutral O cloud morphology, highly peaked at Europa, enhanced downstream of Io where the forward O cloud is located, and is present all around Jupiter at a value in excess of 3×10^4 ions cm^{-2} s^{-1}. The enhanced ion production rates for a downstream angular sector within 90° of Europa and between Io's and Europa's orbits then become volumetrically competitive with the O^+ ion

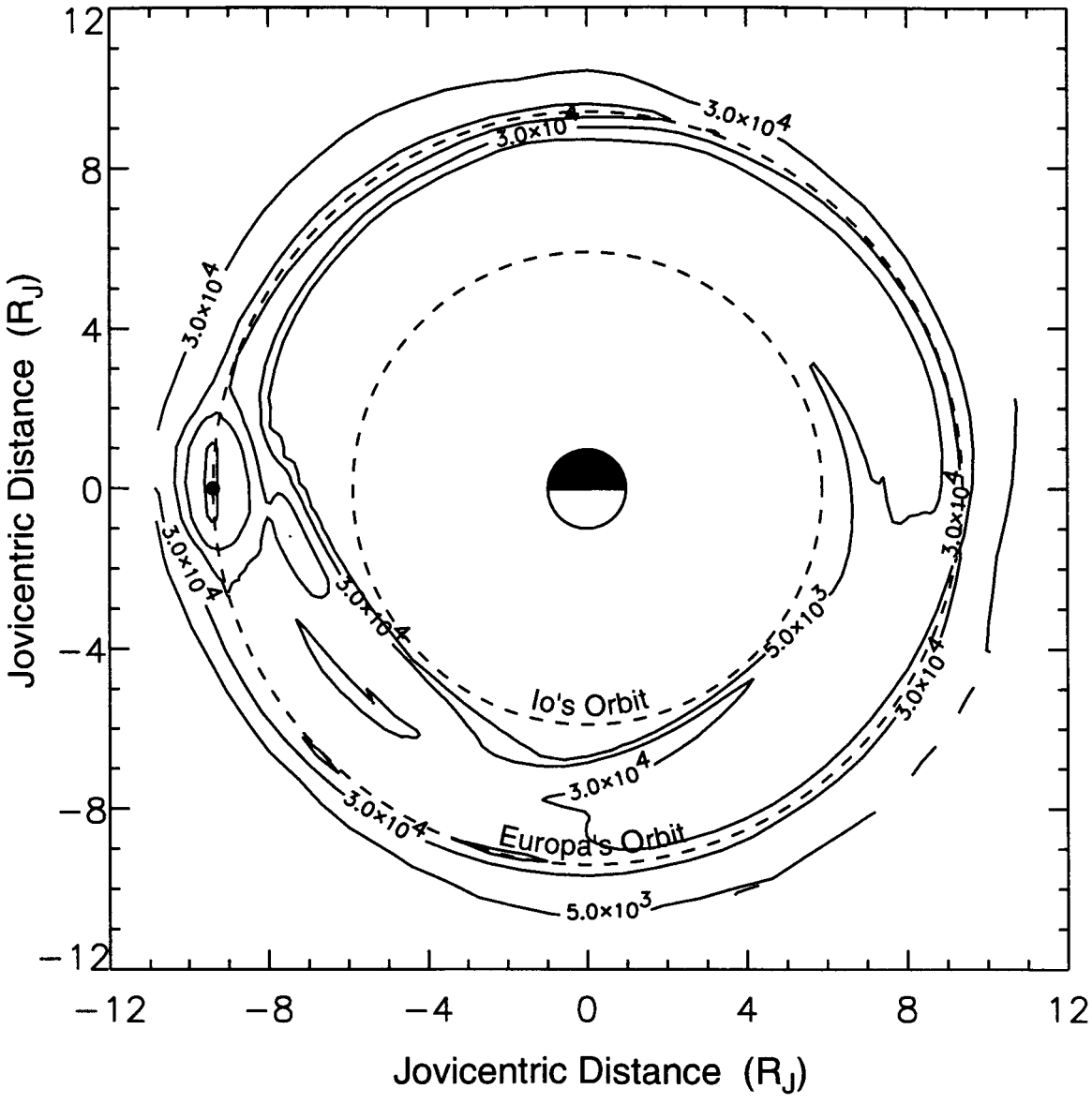

Figure 11. Total O^+ Production Rate for Europa's Atomic Oxygen Clouds. A model calculation for the circumplanetary distribution of the total (EI and CE) instantaneous O^+ production rate (ions cm^{-2} s^{-1}) integrated along the planetary magnetic field that has been produced by Europa's neutral O cloud in Figure 9 is shown. Jupiter and the orbits of Io and Europa are shown to scale. The unmarked contours near Europa are, from outside to inside, 9 x 10^4, 1.5 x 10^5, and 5 x 10^5 ions cm^{-2} s^{-1}.

production rate created by Io's neutral clouds as calculated by Smyth and Marconi (2003). To investigate this competition on a more global scale, radial profiles for the longitudinally-averaged O^+ production rate for EI and CE processes created by the neutral O clouds of Io and

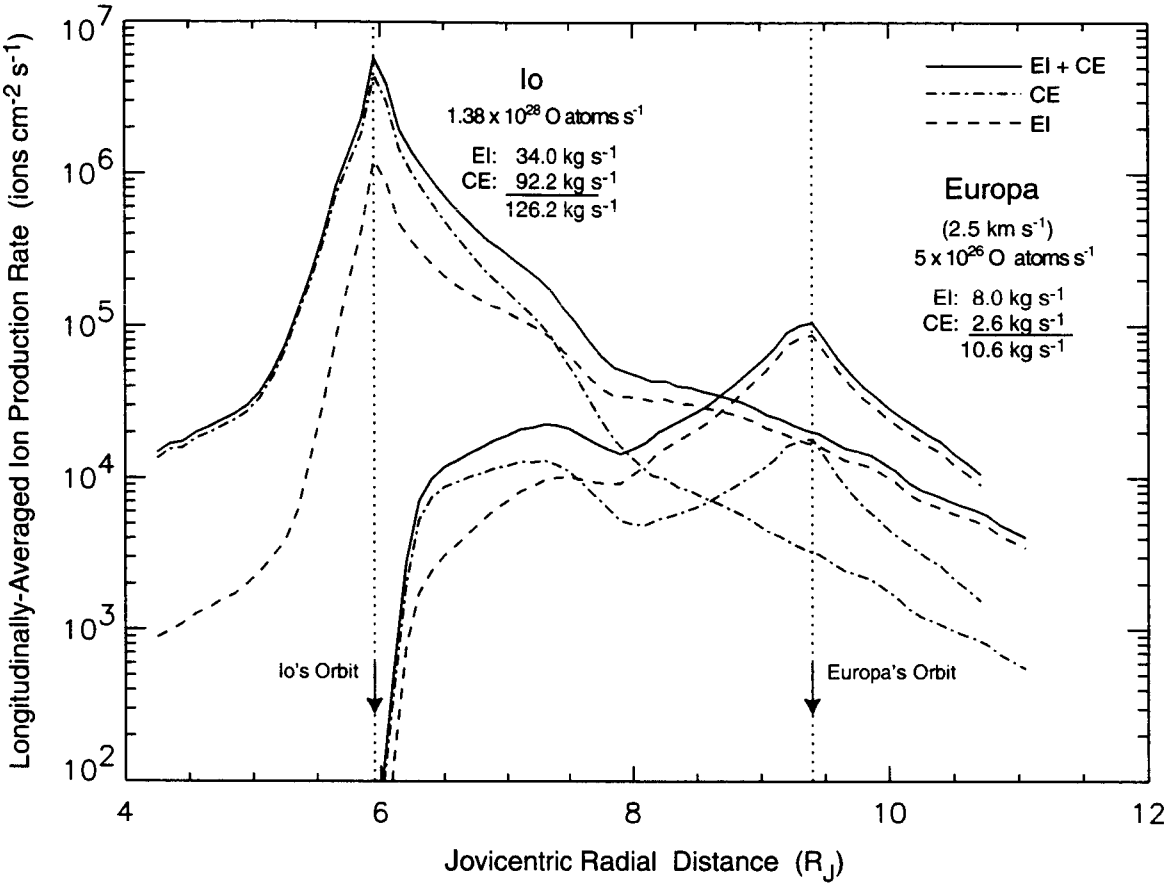

Figure 12. Comparison of the O^+ Production Rate for Io's and Europa's Atomic Oxygen Clouds. Model calculations for the radial profiles of the longitudinally-averaged instantaneous O^+ production rate created by the neutral O clouds of Io and Europa are shown separately for their EI and CE processes in the planetary magnetosphere. The spatially-integrated rates for the separate EI and CE processes are also indicated.

Europa are compared in Figure 12. It can be seen in Figure 12 that the separate EI and CE instantaneous O^+ production rates for Europa are only a factor of 3-4 smaller than the corresponding Io O^+ rates for radial distances at and beyond about 7.5 R_J and that they become equal and larger than the corresponding Io O^+ rates for radial distances at and beyond about 8.75 R_J. It can also be seen from Figure 12 that the CE contribution for the O^+ production rates dominate over the EI contribution near Io's orbit and become equal and then less than the EI rate for radial distances near and beyond about 7 R_J for the Io cloud and near and beyond about 8 R_J for the Europa cloud. This occurs because the electron temperature increases significantly for larger radial distances outside of Io's orbit and becomes the dominant loss mechanism for neutrals. In addition to mass loading rates from the O neutral cloud, Europa also supplies a direct loss of O_2^+ pickup ions with a rate of ~1 x 10^{26} s^{-1} (or 5.3 kg s^{-1}).

References

Bagenal, F. (1994) Empirical Model of the Io Plasma Torus: Voyager Measurements, *J. Geophys. Res.* **99**, 11043-11062.

33

Dalgarno A., M. Yan, and W. Liu (1999) Electron Energy Deposition in a Gas Mixture of Atomic and Molecular Hydrogen and Helium, *Ap. J. Supp.* **125**, 237-256.

Garrett B.C., L.T. Redmon, C.W. McCurdy, and M. Redmon (1985) Electronic Excitation and Dissociation of O_2 and S_2 by Electron Impact, *Phys. Rev. A* **32**, 3366-3375.

Hall, D.T., P.D. Feldman, M.A. McGrath, and D.F. Strobel (1998) The Far-Ultraviolet Oxygen Airglow of Europa and Ganymede, *Ap. J.* **499**, 475-481.

Hall, D.T., D.F. Strobel, P.D. Feldman, M.A. McGrath, and H.A. Weaver (1995) Detection of an Oxygen Atmosphere on Jupiter's Moon Europa, *Nature* **373**, 677-679.

Hubner, W.F., J.J. Keady, and S.P. Lyon (1992) Solar Photo Rates for Planetary Atmospheres and Atmospheric Pollutants, Kluwer Academic Publishers, Boston.

Jacobson, R. A. (2001) Gravity Field of the Jovian System and the Orbits of the Regular Jovian Satellites, *BAAS* **33**, No. 3, 1039.

Johnson, R.E. and T.I. Quickenden, P.D. Cooper, A.J. McKinley, and C.G. Freeman (2004) The Production of Oxidants in Europa's Surface, preprint.

Krishnakumar E. and S.K. Srivastava (1992) Cross-sections for Electron Impact Ionization of O_2, *International Journal of Mass Spectrometry and Ion Processes* **113**, 1-12.

Mauk, B.H., D.G. Mitchell, S.M. Krimigis, E.C. Roelof, and C.P. Paranicas (2003) Energetic Neutral Atoms from a Trans-Europa Gas Torus at Jupiter, *Nature* **421**, 920-922.

Peale, S.J., P. Cassen, and R.T. Reynolds (1979) Melting of Io by Tidal Dissipation, *Science* **203**, 892-894.

Saur, J., D.F. Strobel, and F.M. Neubauer (1998) Interaction of the Jovian Magnetosphere with Europa: Constraints on the Neutral Atmosphere, *J. Geophys. Res.* **103**, 19,947-19,962.

Shematovich, V.I. and R.E. Johnson (2001) Near-Surface Oxygen Atmosphere at Europa, *Adv. Space Res.* **27**, 1881-1888.

Shematovich, V.I., R.E. Johnson, J.F. Cooper and M.C. Wong (2004) Surface-Bound Atmosphere of Europa, preprint.

Shirai T., T. Tabata. and H. Tawara (2001) Analytic Cross-sections for Electrons Collisions with CO, CO_2, and H_2O Relevant to Fusion Edge Plasma Impurities, *ATNDT* **79**, 143-184.

Smyth, W.H. and M.L. Marconi (2003) Nature of the Iogenic Plasma Source in Jupiter's Magnetosphere I. Circumplanetary Distribution, *Icarus*, **166**, 85-106.

Smyth, W.H. and M.L. Marconi (2004) Europa's Atmosphere and its Impact on Jupiter's Magnetosphere, paper in preparation.

Stibbe D.T. and J. Tennyson (1999) Rates for the Electron Impact Dissociation and Molecular Hydrogen, *Ap. J. Letts.* **513**, L147-L150.

Straub H.C., P. Renault, B.G. Lindsay, K.A. Smith, and R.F. Stebbings (1996) Absolute Partial Cross-Sections for Electron-Impact Ionization of H_2, N_2, and O_2 from threshold to 1000 eV, *Phys. Rev. A* **54**, 2146-2152.

Wakiya, K. (1978) Differential and Integral Cross-Sections for the Electron Impact Excitation of O_2. 1. Optically Allowed Transitions from the Ground State, *J. Phys. B* **11**, 3913-3930.

Woodward, R.C. and W.H. Smyth (1994) Modeling the Io Plasma Torus: Effects of Global Parameters, *BAAS* **26**, 1139.

REPORT DOCUMENTATION PAGE

Form Approved
OMB No. 0704-0188

1. AGENCY USE ONLY *(Leave blank)*	2. REPORT DATE	3. REPORT TYPE AND DATES COVERED
	April 7, 2004	Final, February 19 , 2002 to February 18, 2004

4. TITLE
Studies for the Europagenic Plasma Source in Jupiter's Inner Magnetosphere during the Galileo Europa Mission

5. FUNDING NUMBERS
NASW-02003

6. AUTHORS
William H. Smyth

7. PERFORMING ORGANIZATION NAME(S) AND ADDRESS(ES)
Atmospheric and Environmental Research, Inc.
131 Hartwell Avenue
Lexington, MA 02421

8. PERFORMING ORGANIZATION REPORT NUMBER
P-880

9. SPONSORING/MONITORING AGENCY NAME(S) AND ADDRESS(ES)
NASA Headquarters
Headquarters Contract Division
Washington, DC 20546

10. SPONSORING/MONITORING AGENCY REPORT NUMBER

11. SUPPLEMENTARY NOTES

12a. DISTRIBUTION/AVAILABILITY STATEMENT

12b. DISTRIBUTION CODE

13. ABSTRACT *(Maximum 200 words)*

Progress in research to understand the three-dimensional nature of the Europagenic plasma torus is summarized. Efforts to improve the plasma torus description near Europa's orbit have included a better understanding of Europa's orbit and an improved description of the planetary magnetic field. New plasma torus chemistry for molecular and atomic species has been introduced and implemented in Europa neutral cloud models. Preliminary three-dimensional model calculations for Europa's neutral clouds and their plasma sources are presented.

14. SUBJECT TERMS
Io, satellite atmospheres

15. NUMBER OF PAGES
27

16. PRICE CODE

17. SECURITY CLASSIFICATION OF REPORT	18. SECURITY CLASSIFICATION OF THIS PAGE	19. SECURITY CLASSIFICATION OF ABSTRACT	20. LIMITATION OF ABSTRACT
Unclassified	Unclassified	Unclassified	Unlimited

NSN 7540-01-280-5500 Computer Generated STANDARD FORM 298 (Rev 2-89)
Prescribed by ANSI Std 239-18
298-102